



# Optimization of Yttrium Doping for Barium Fluoride Crystals with Suppressed Slow Scintillation Component

Chen Hu<sup>a</sup>, Chao Xu<sup>b</sup>, Fan Yang<sup>a,c</sup>, Liyuan Zhang<sup>a</sup>,  
Qinghui Zhang<sup>b</sup> and Ren-Yuan Zhu<sup>a</sup>

<sup>a</sup> *California Institute of Technology, 1200 E California Blvd, Pasadena, CA 91125, USA*

<sup>b</sup> *Beijing Scitlion Technology Corp., Ltd., No 5 Xingguang 4 Ave, Beijing, China, 101111*

<sup>c</sup> *Nankai University, 94 South Weijin Road, Tianjin, China, 300071*

October 26, 2017

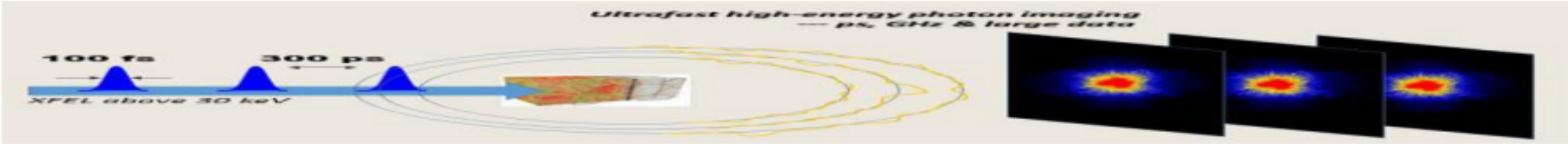


# Fast & Radiation Hard Scintillators

- Supported by the DOE HEP advanced detector R&D program we are developing fast and radiation hard inorganic scintillators to face the challenge for future HEP experiments at the energy and intensity frontiers.
- Our investigation shows that  $\text{LYSO:Ce}$ ,  $\text{BaF}_2$  and  $\text{LuAG:Ce}$  will survive the radiation environment expected at the HL-LHC with  $3,000 \text{ fb}^{-1}$ .  $\text{LYSO}$  is proposed for a precision MIP Timing Detector for the CMS Phase-II upgrade for the HL-LHC:
  - Ionizations dose: up to 100 Mrad,
  - Charged hadron fluence: up to  $6 \times 10^{14} \text{ p/cm}^2$ ,
  - Fast neutron fluence: up to  $3 \times 10^{15} \text{ n/cm}^2$ .
- Ultra-fast scintillators with excellent radiation hardness is also needed to face the challenge of unprecedented event rate expected by future HEP experiments at the intensity frontier, such as Mu2e-II, and the GHz hard X-ray imaging for the proposed Marie project at Los Alamos National Laboratory.
- Yttrium doped  $\text{BaF}_2$  with a sub-ns FWHM pulse width and a suppressed slow scintillation component is a leading candidate for both applications.



# GHz Hard X-Ray Imaging for Marie



## High-Energy and Ultrafast X-Ray Imaging Technologies and Applications

Organizers: Peter Denes, Sol Gruner, Michael Stevens & Zhehui (Jeff) Wang<sup>1</sup>  
 (Location/Time: Santa Fe, NM, USA /Aug 2-3, 2016)

The goals of this workshop are to gather the leading experts in the related fields, to prioritize tasks for ultrafast hard X-ray imaging detector technology development and applications in the next 5 to 10 years, see Table 1, and to establish the foundations for near-term R&D collaborations.

Table I. High-energy photon imagers for MaRIE XFEL

Performance	Type I imager	Type II imager
X-ray energy	30 keV	42-126 keV
Frame-rate/inter-frame time	0.5 GHz/2 ns	3 GHz / 300 ps
Number of frames	10	10 - 30
X-ray detection efficiency	above 50%	above 80%
Pixel size/pitch	$\leq 300 \mu\text{m}$	$< 300 \mu\text{m}$
Dynamic range	$10^3$ X-ray photons	$\geq 10^4$ X-ray photons
Pixel format	64 x 64 (scalable to 1 Mpix)	1 Mpix

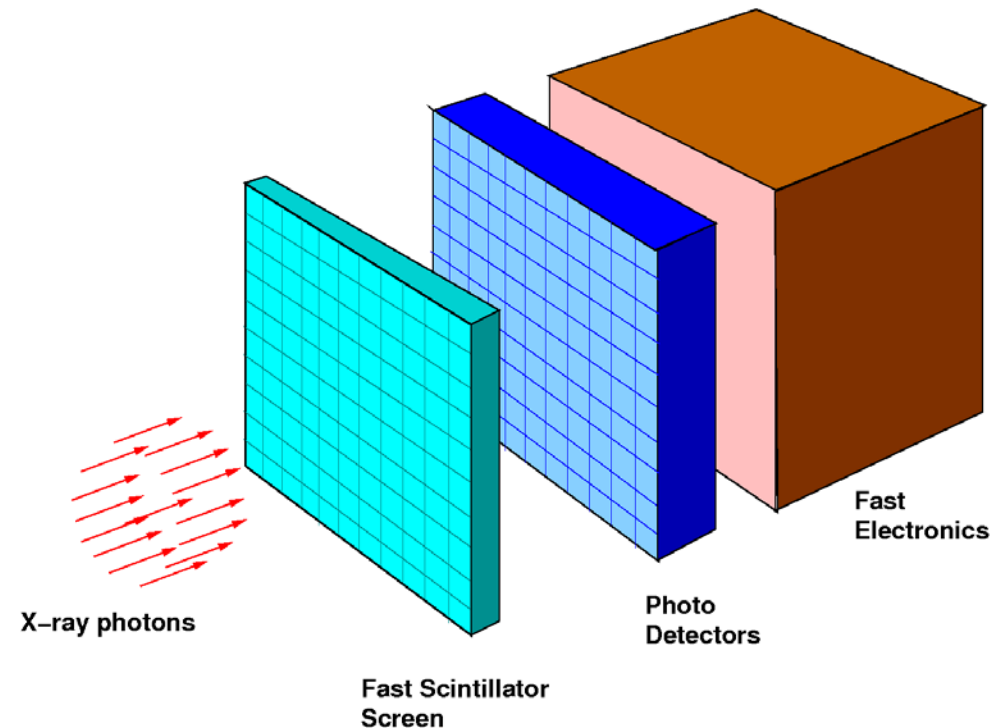
2 ns and 300 ps inter-frame time requires very fast sensor



# Why Crystal Scintillator?



- Detection efficiency for hard X-ray requires bulk detector.
- Scintillation light provides fastest signal.
- Pixelized crystal detector is a standard in medical industry.
- A total absorption imager:
  - Pixelized fast scintillator screen;
  - Pixelized fast photodetector;
  - Fast electronics readout.
- Challenges:
  - Ultra fast scintillator;
  - Ultra fast photodetector;
  - Ultra fast readout electronics.

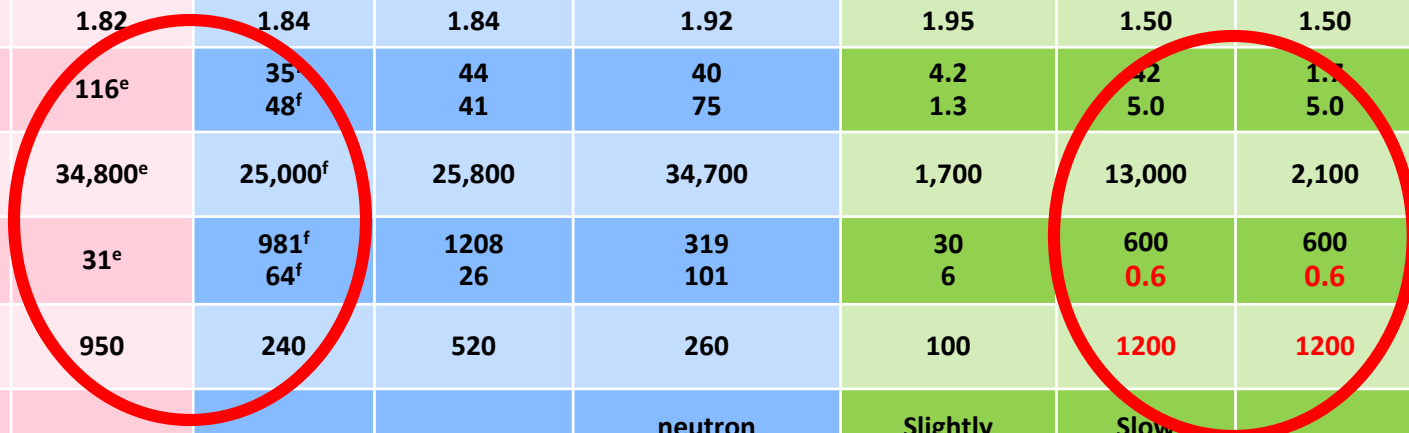




# Fast Inorganic Scintillators for HEP



	LSO:Ce	LYSO:Ce,Ca <sup>[1]</sup>	LuAG:Ce <sup>[2]</sup>	LuAG:Pr <sup>[3]</sup>	GGAG:Ce <sup>[4,5]</sup>	CsI	BaF <sub>2</sub> <sup>[6]</sup>	BaF <sub>2</sub> :Y	CeBr <sub>3</sub>	LaBr <sub>3</sub> :Ce <sup>[7]</sup>
Density (g/cm <sup>3</sup> )	7.4	7.4	6.76	6.76	6.5	4.51	4.89	4.89	5.23	5.29
Melting points (°C)	2050	2050	2060	2060	1850 <sup>d</sup>	621	1280	1280	722	783
X <sub>0</sub> (cm)	1.14	1.14	1.45	1.45	1.63	1.86	2.03	2.03	1.96	1.88
R <sub>M</sub> (cm)	2.07	2.07	2.15	2.15	2.20	3.57	3.1	3.1	2.97	2.85
λ <sub>1</sub> (cm)	20.9	20.9	20.6	20.6	21.5	39.3	30.7	30.7	31.5	30.4
Z <sub>eff</sub>	64.8	64.8	60.3	60.3	51.8	54.0	51.6	51.6	45.6	45.6
dE/dX (MeV/cm)	9.55	9.55	9.22	9.22	8.96	5.56	6.52	6.52	6.65	6.90
λ <sub>peak</sub> <sup>a</sup> (nm)	420	420	520	310	540	310	300 220	300 220	371	360
PL Emission Peak (nm)	402	402	500	308	540	310	300 220	300 220	350	360
PL Excitation Peak (nm)	358	358	450	275	445	256	<200	<200	330	295
Absorption Edge (nm)	170	170	160	160	190	200	140	140	n.r.	220
Refractive Index <sup>b</sup>	1.82	1.82	1.84	1.84	1.92	1.95	1.50	1.50	1.9	1.9
Normalized Light Yield <sup>a,c</sup>	100	116 <sup>e</sup>	35 <sup>e</sup> 48 <sup>f</sup>	44 41	40 75	4.2 1.3	4.2 5.0	1.7 5.0	99	153
Total Light yield (ph/MeV)	30,000	34,800 <sup>e</sup>	25,000 <sup>f</sup>	25,800	34,700	1,700	13,000	2,100	30,000	46,000
Decay time <sup>a</sup> (ns)	40	31 <sup>e</sup>	981 <sup>f</sup> 64 <sup>f</sup>	1208 26	319 101	30 6	600 0.6	600 0.6	17	20
Light Yield in 1 <sup>st</sup> ns (photons/MeV)	740	950	240	520	260	100	1200	1200	1,700	2,200
Issues					neutron x-section	Slightly hygroscopic	Slow component	DUV PD	hygroscopic	





# Fast Inorganic Scintillators (II)



- a. Top line: slow component, bottom line: fast component;
- b. At the wavelength of the emission maximum;
- c. Excited by Gamma rays;
- d. For  $\text{Gd}_3\text{Ga}_3\text{Al}_2\text{O}_{12}:\text{Ce}$
- e. For 0.4 at% Ca co-doping
- f. Ceramic with 0.3 Mg at% co-doping
- g. Defined as LY(2 to 4 ns)/LY(0 to 2 ns)

- [1] Spurrier, et al., *IEEE T. Nucl. Sci.* 2008,55 (3): 1178-1182
- [2] Liu, et al., *Adv. Opt. Mater.* 2016, 4(5): 731–739
- [3] Hu, et al., *Phys. Rev. Applied* 2016, 6: 064026
- [4] Lucchini, et al., *NIM A* 2016, 816: 176-183
- [5] Meng, et al., *Mat. Sci. Eng. B-Solid* 2015, 193: 20-26
- [6] Diehl, et al., *J. Phys. Conf. Ser* 2015, 587: 012044
- [7] Pustovarov, et al., *Tech. Phys. Lett.* 2012, 784-788

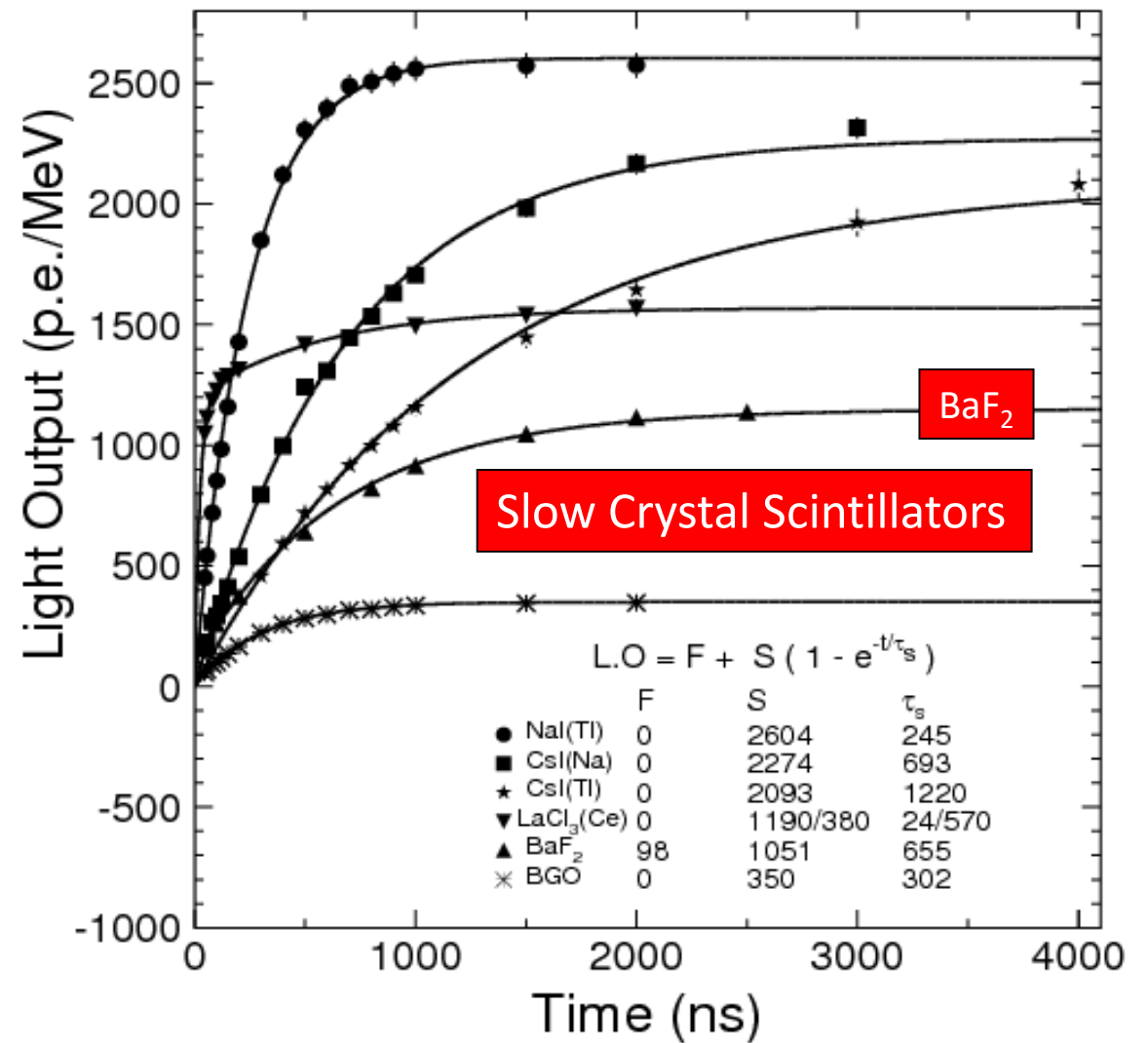
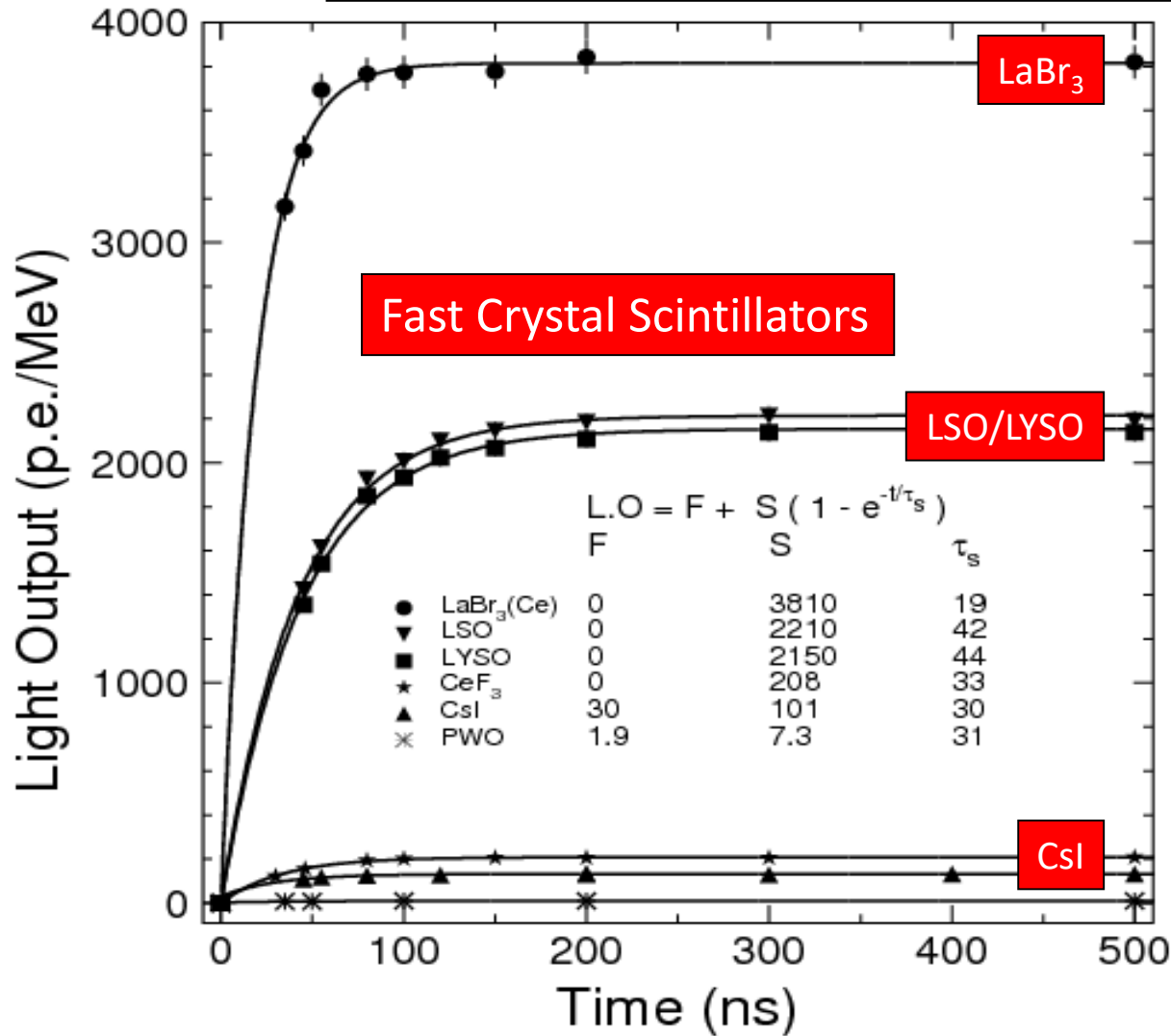




# Light Output & Decay Kinetics



Measured with Philips XP2254B PMT (multi-alkali cathode)  
 p.e./MeV: LSO/LYSO is 6 & 230 times of BGO & PWO respectively

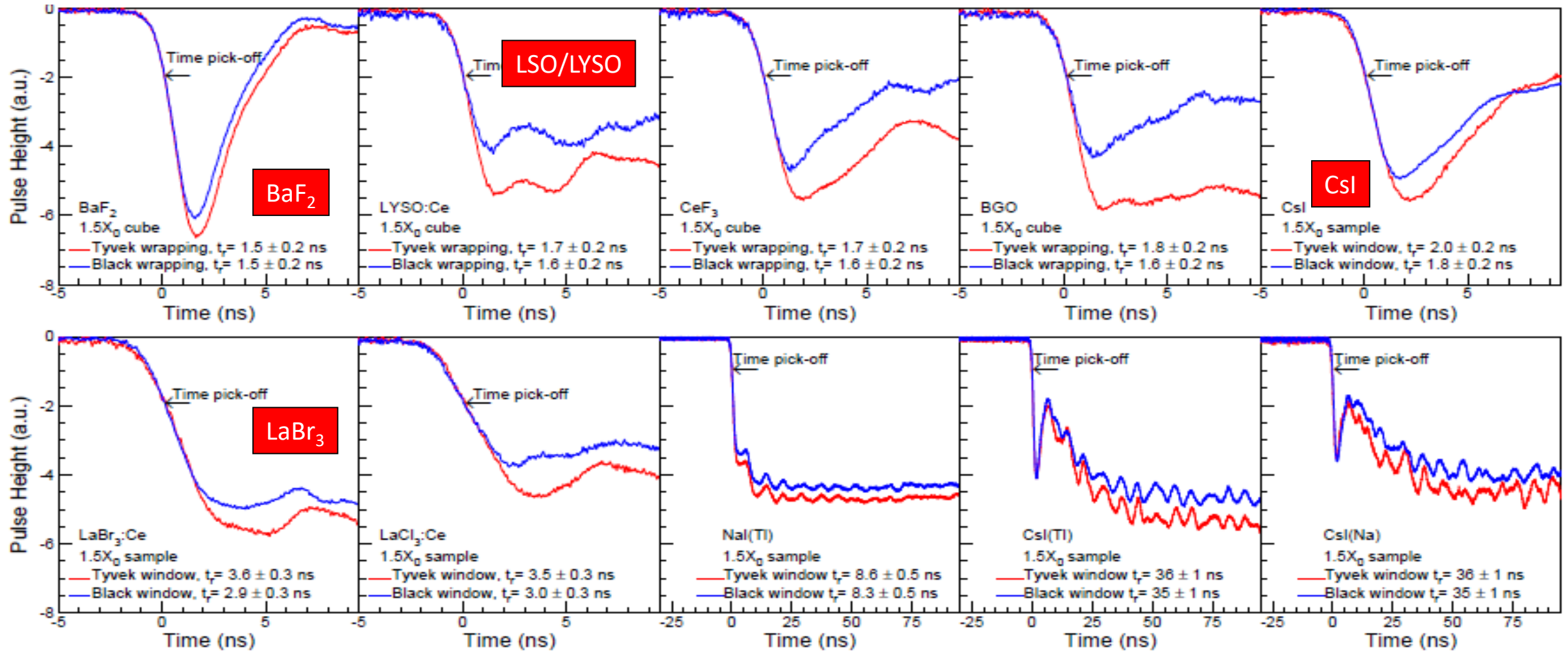




# Scintillation Pulses: $1.5 X_0$ Crystals



Hamamatsu R2059 PMT (2500 V)/Agilent MSO9254A (2.5 GHz) DSO with 1.3/0.14 ns rise time



The 3 ns FWHM pulse width of BaF<sub>2</sub> will be reduced by using a faster photodetector  
LYSO, LaBr<sub>3</sub> & CeBr<sub>3</sub> have tail, which would cause pile-up for GHz hard X-ray imaging





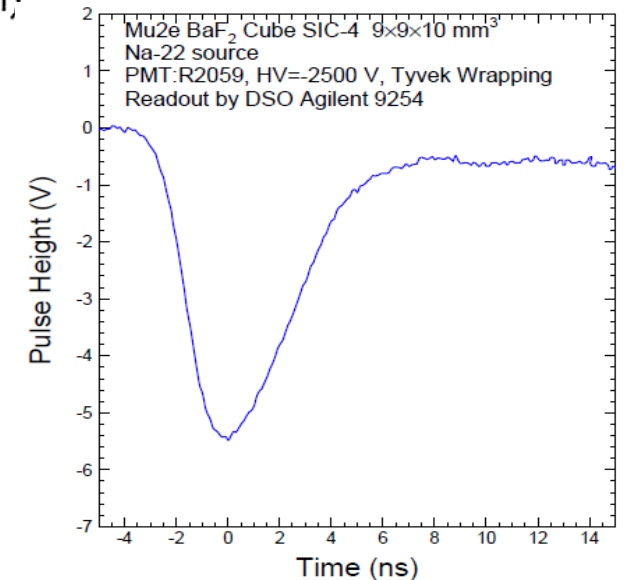
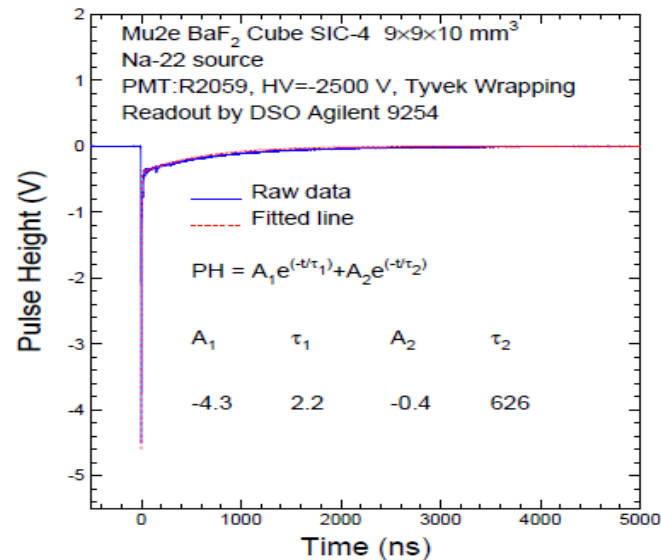
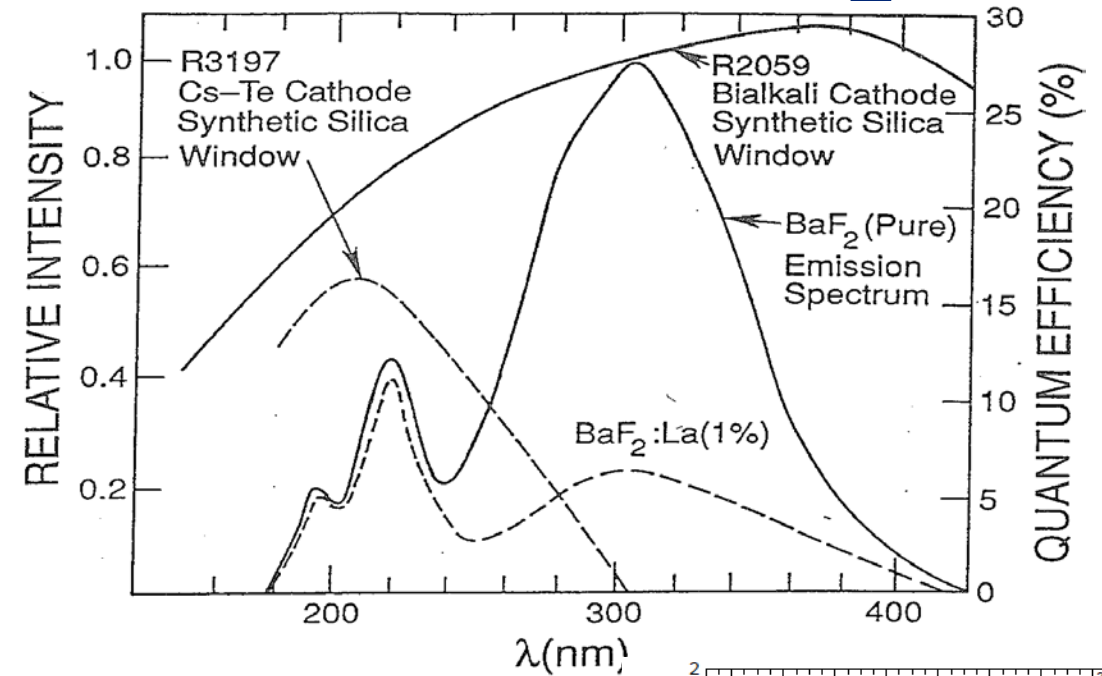
# Fast and Slow Light from BaF<sub>2</sub>



BaF<sub>2</sub> has a fast scintillation component with sub-ns decay time, and a slow component with 600 ns decay time.

The amount of the fast light is similar to undoped CsI, and is 1/5 of the slow component.

Spectroscopic selection of the fast component may be realized by selective doping with rare earths and/or a solar blind photodetector.



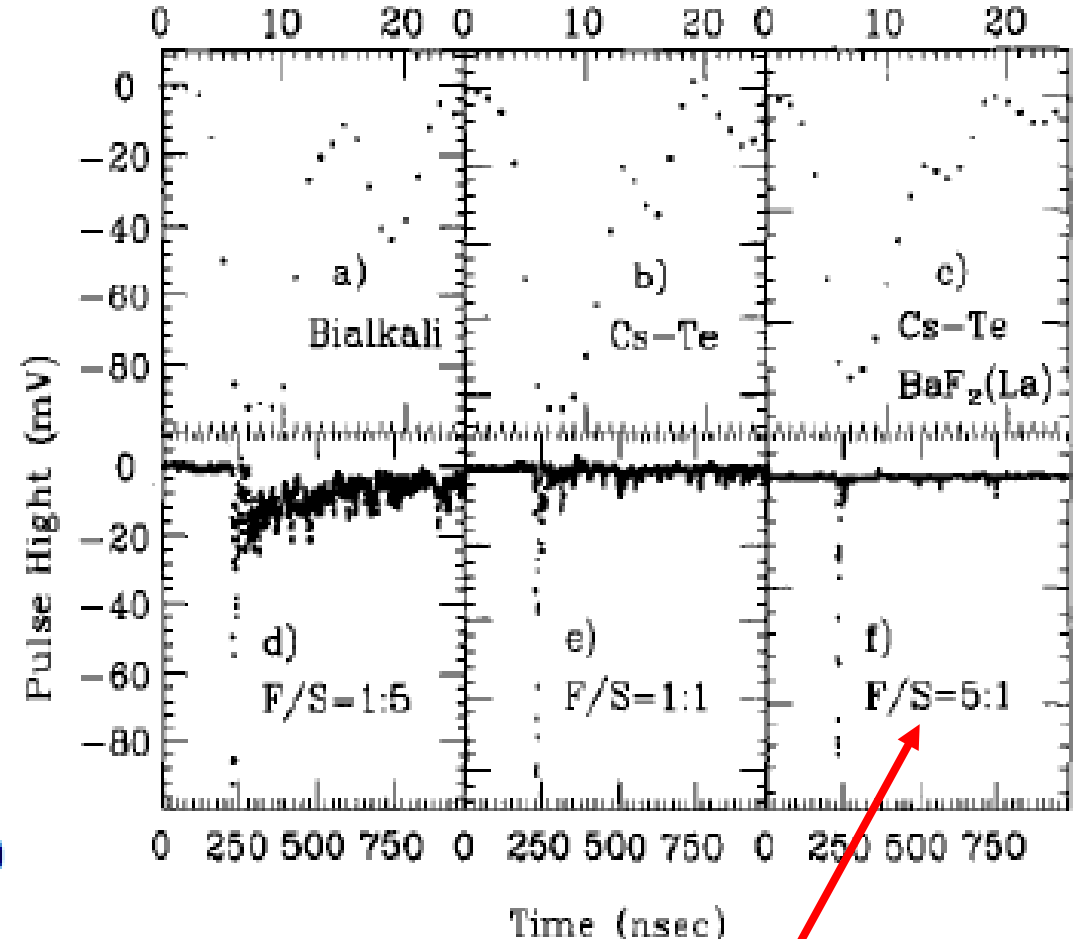
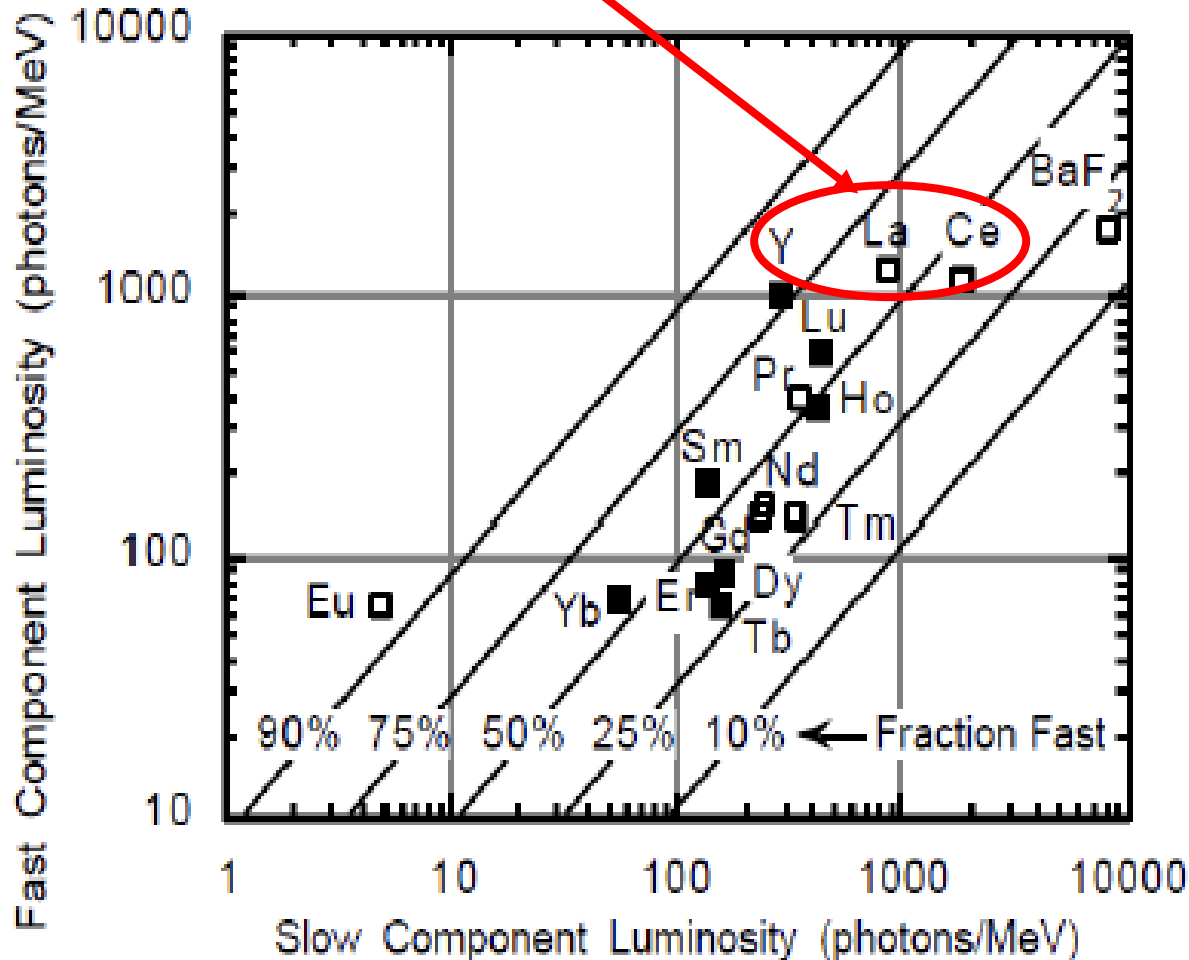


# Slow Suppression: Doping & Readout



Slow component may be suppressed by RE doping: Y, La and Ce

B.P. SOBOLEV et al., "SUPPRESSION OF BaF<sub>2</sub> SLOW COMPONENT OF X-RAY LUMINESCENCE IN NON-STOICHIOMETRIC Ba<sub>0.9R0.1</sub>F<sub>2</sub> CRYSTALS (R=RARE EARTH ELEMENT)," *Proceedings of The Material Research Society: Scintillator and Phosphor Materials*, pp. 277-283, 1994.



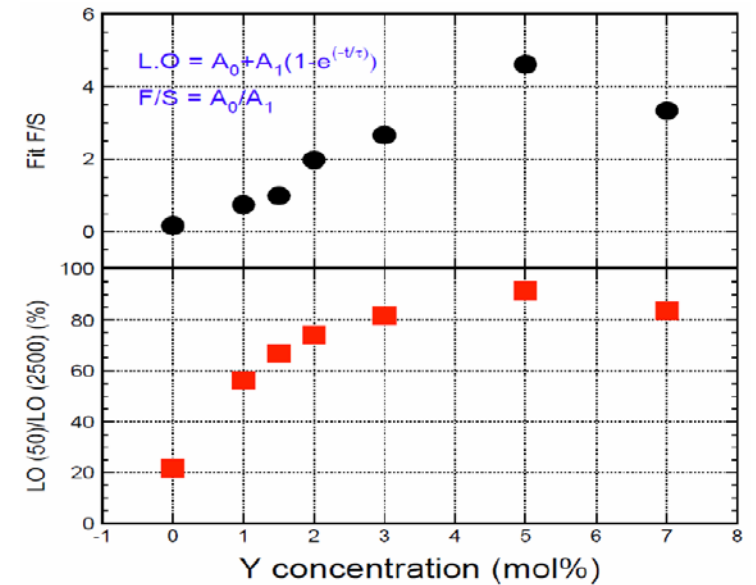
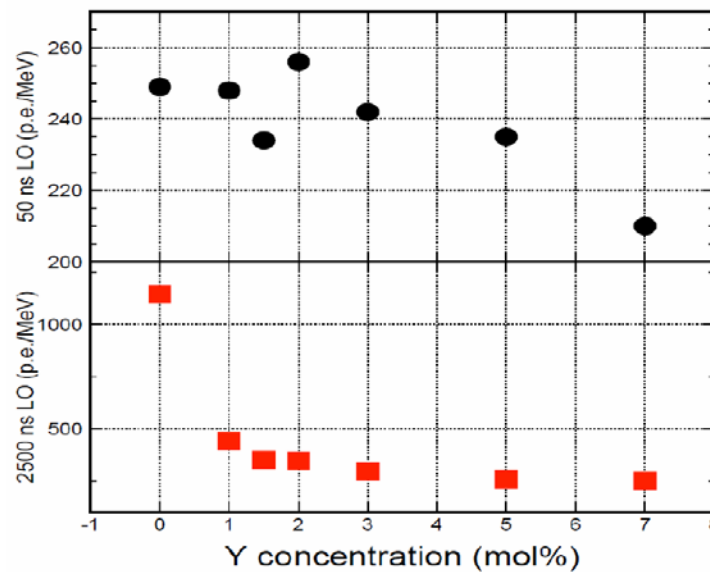
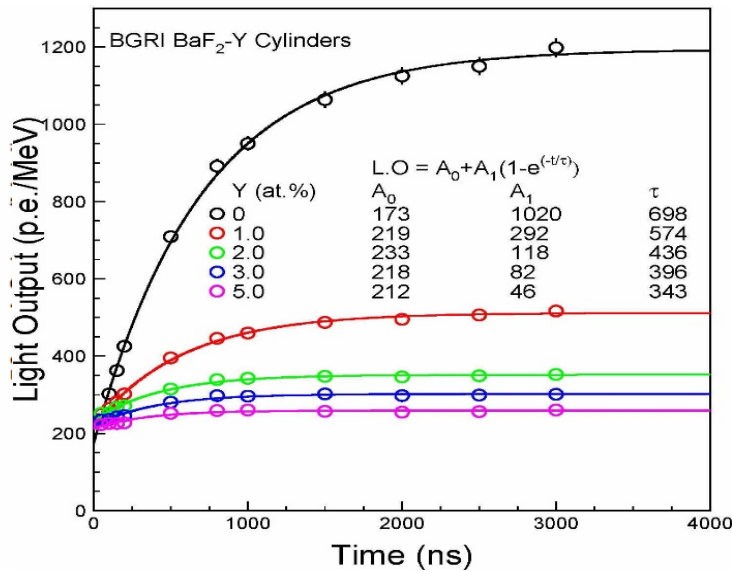
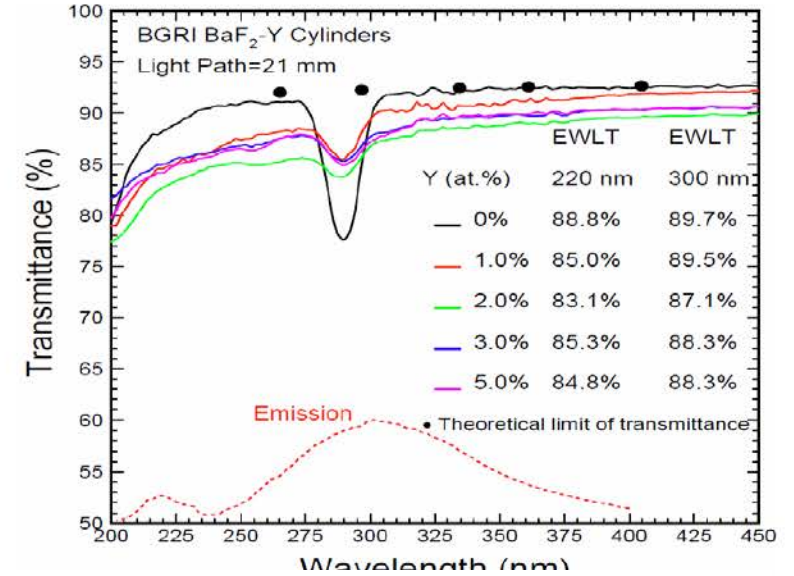
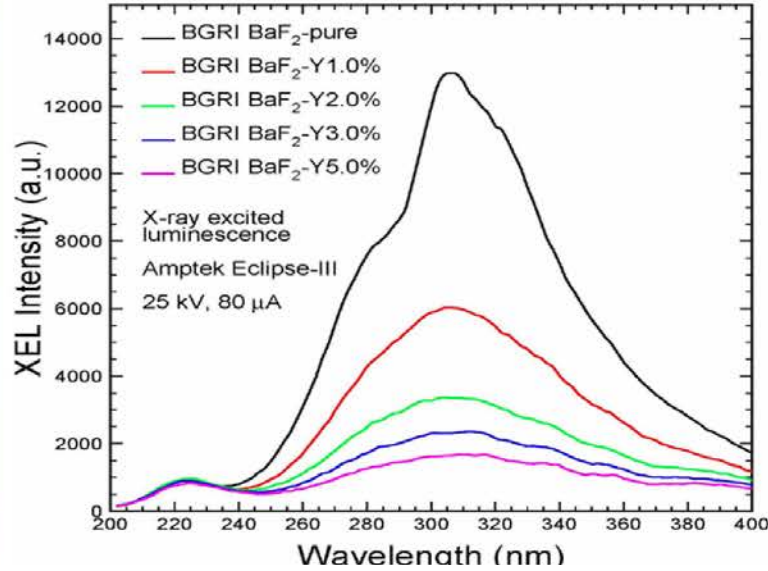
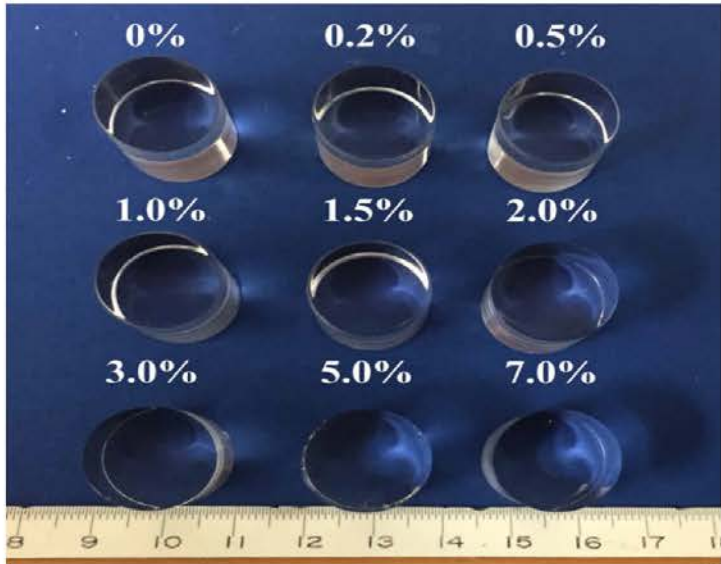
Solar-blind cathode (Cs-Te) and La doping achieved F/S = 5/1



# Optimization of Yttrium Doping in BaF<sub>2</sub>



F/S ratio from 1/5 to 5/1, presented in TIPP 2017, Beijing

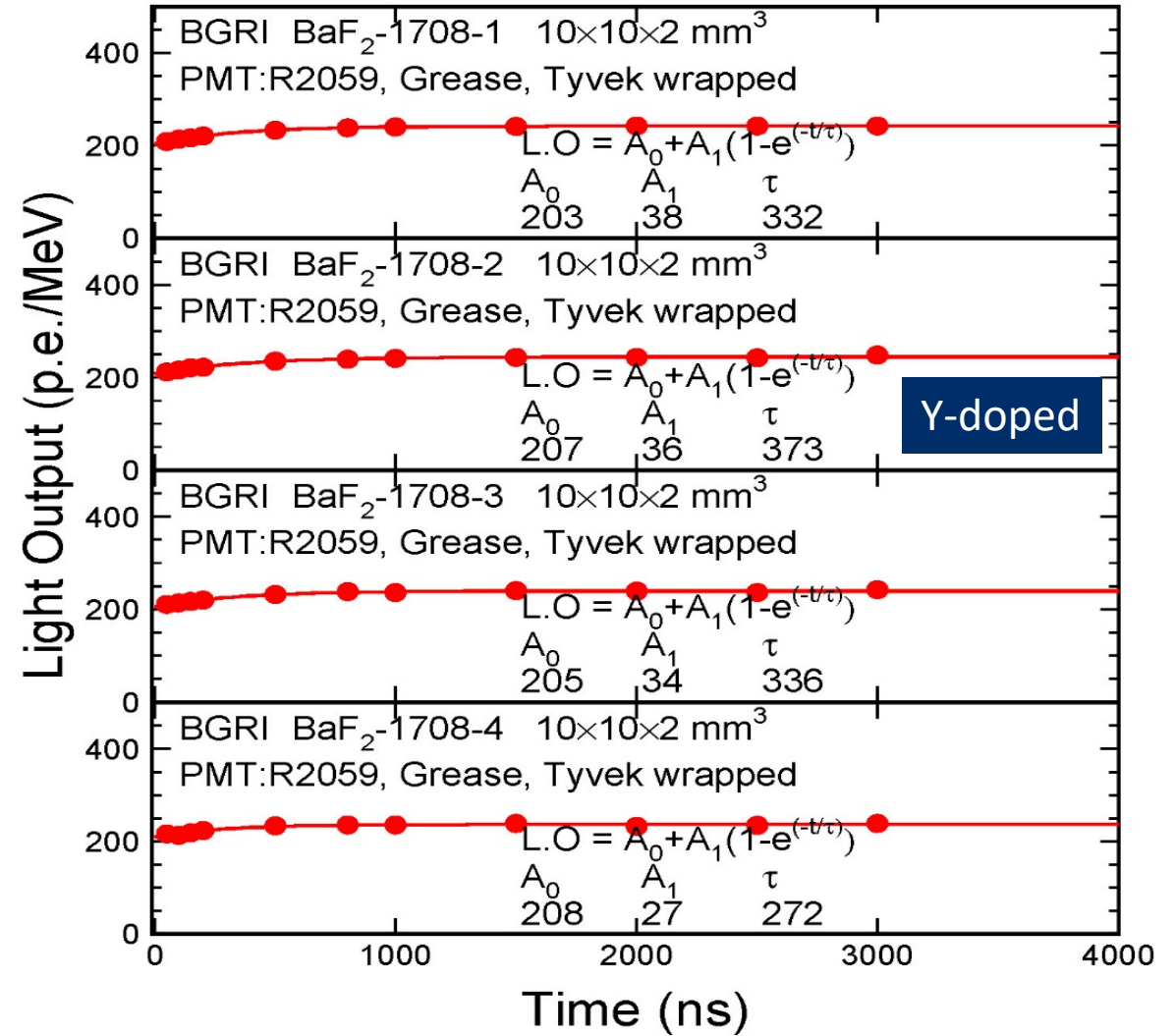
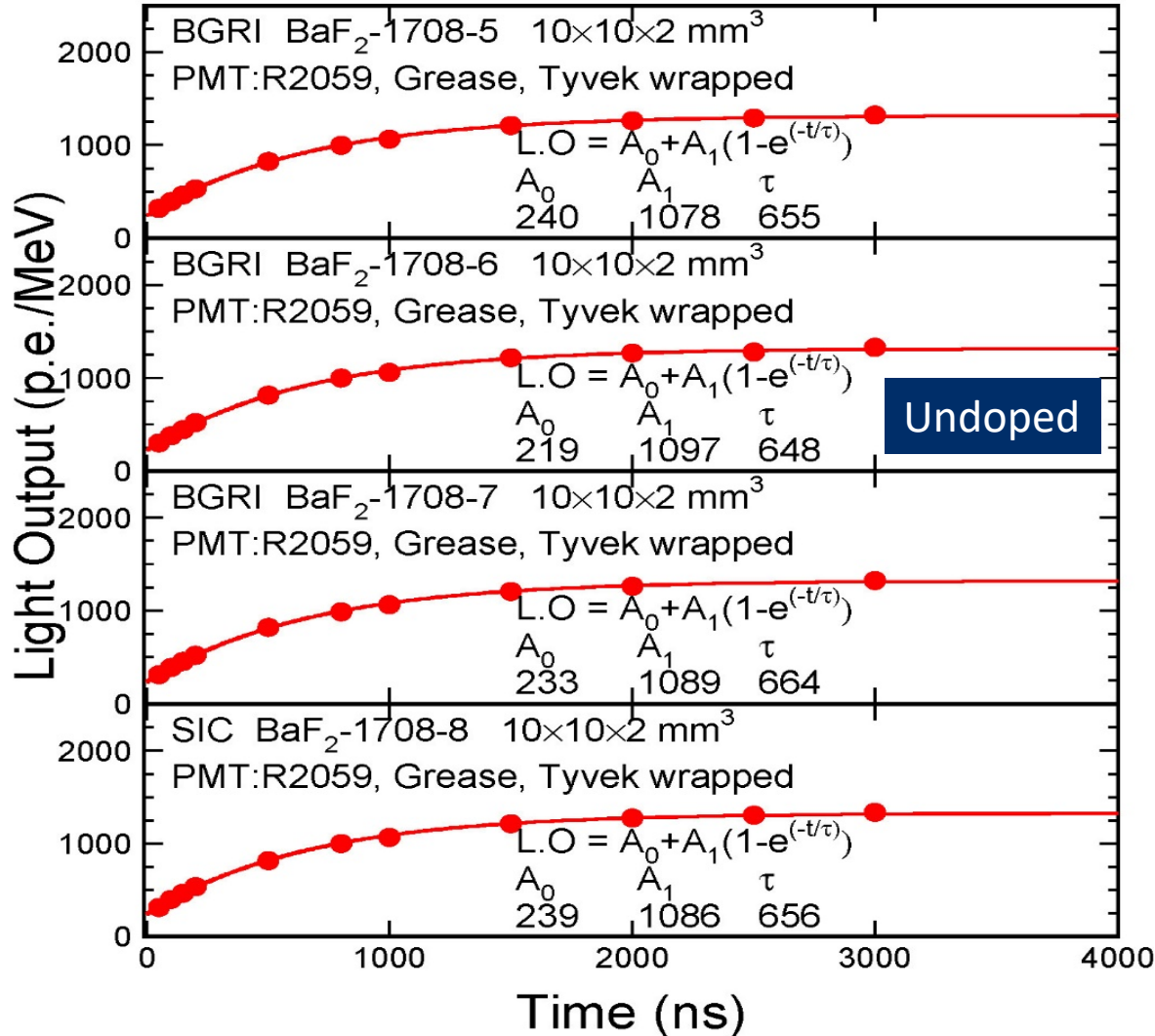




# Optimized Y Doping in BaF<sub>2</sub>



F/S ratio increased from 0.21 to 6.2



Samples are being irradiation up to 200 Mrad and  $2 \times 10^{15}$  n/cm<sup>2</sup> in East Port of LANSCE

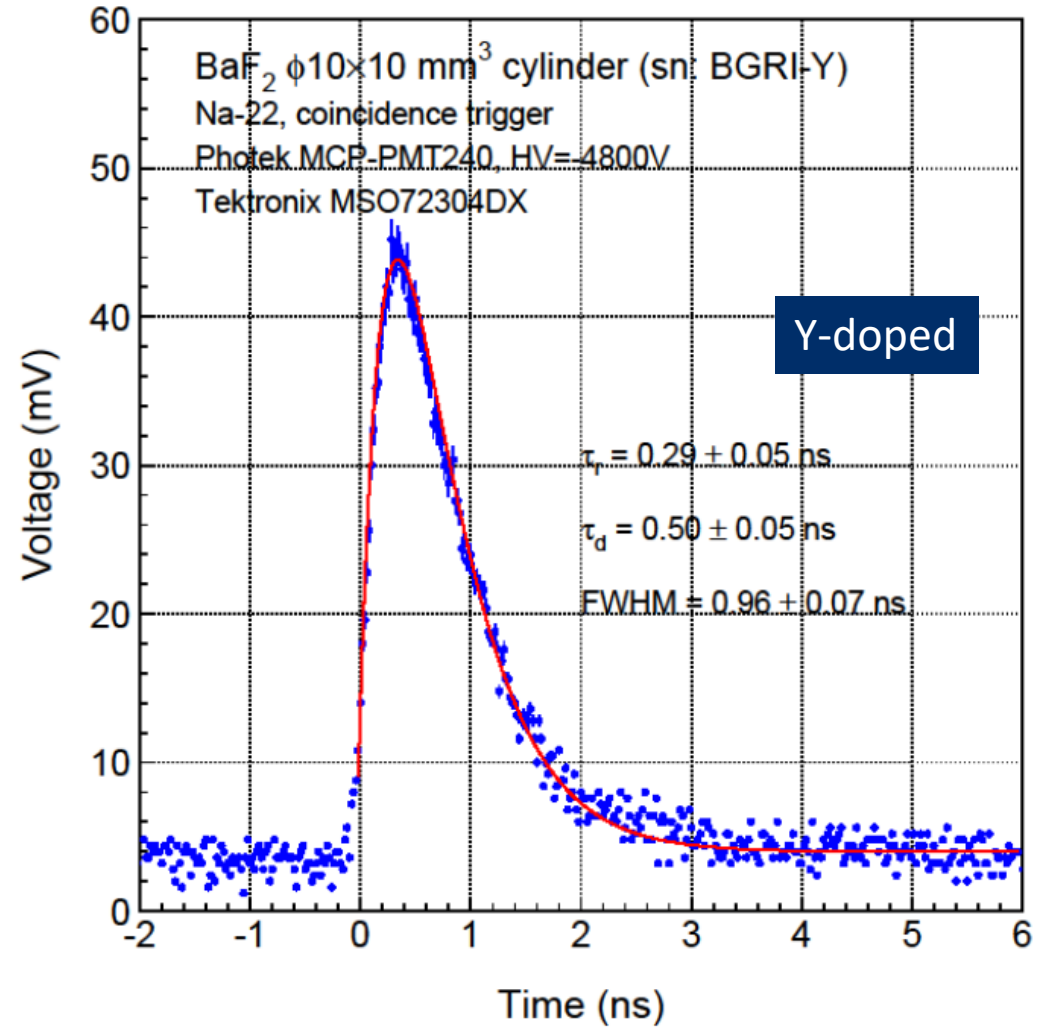
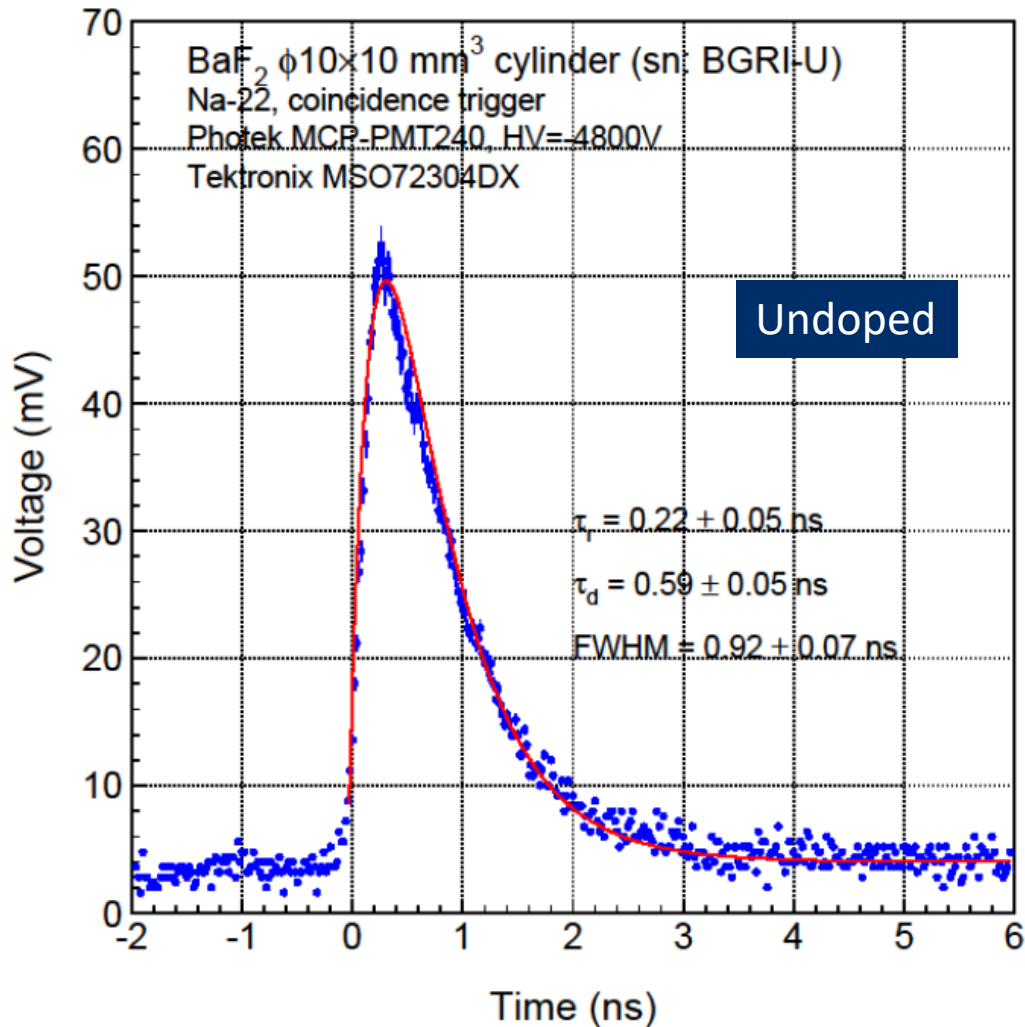




# Pulse Shape: BaF<sub>2</sub> Cylinders



BGRI BaF<sub>2</sub> cylinders of  $\Phi 10 \times 10$  mm<sup>3</sup> shows  $\gamma$ -ray response:  
0.26/0.55/0.94 ns of rising/decay/FWHM width

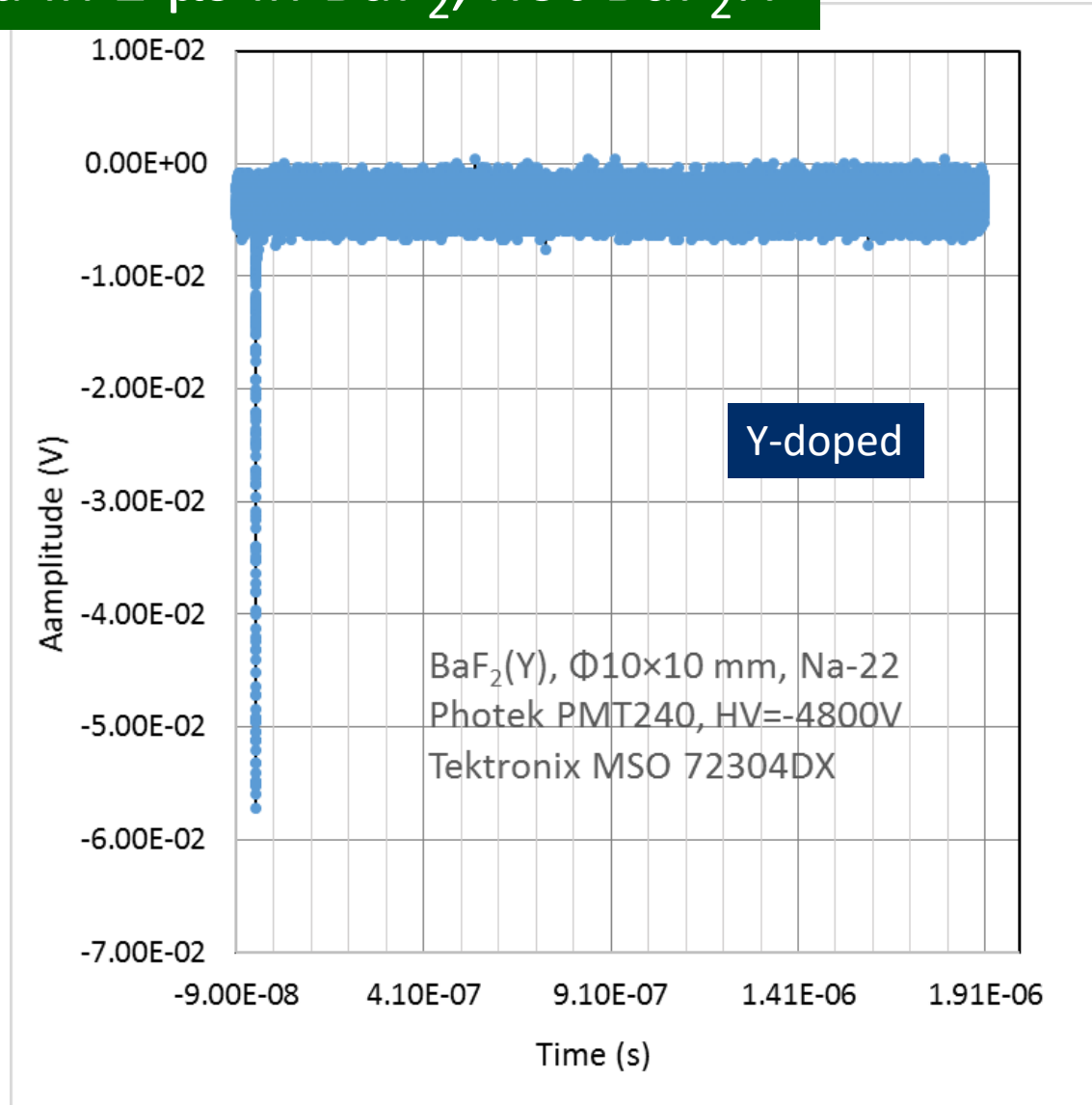
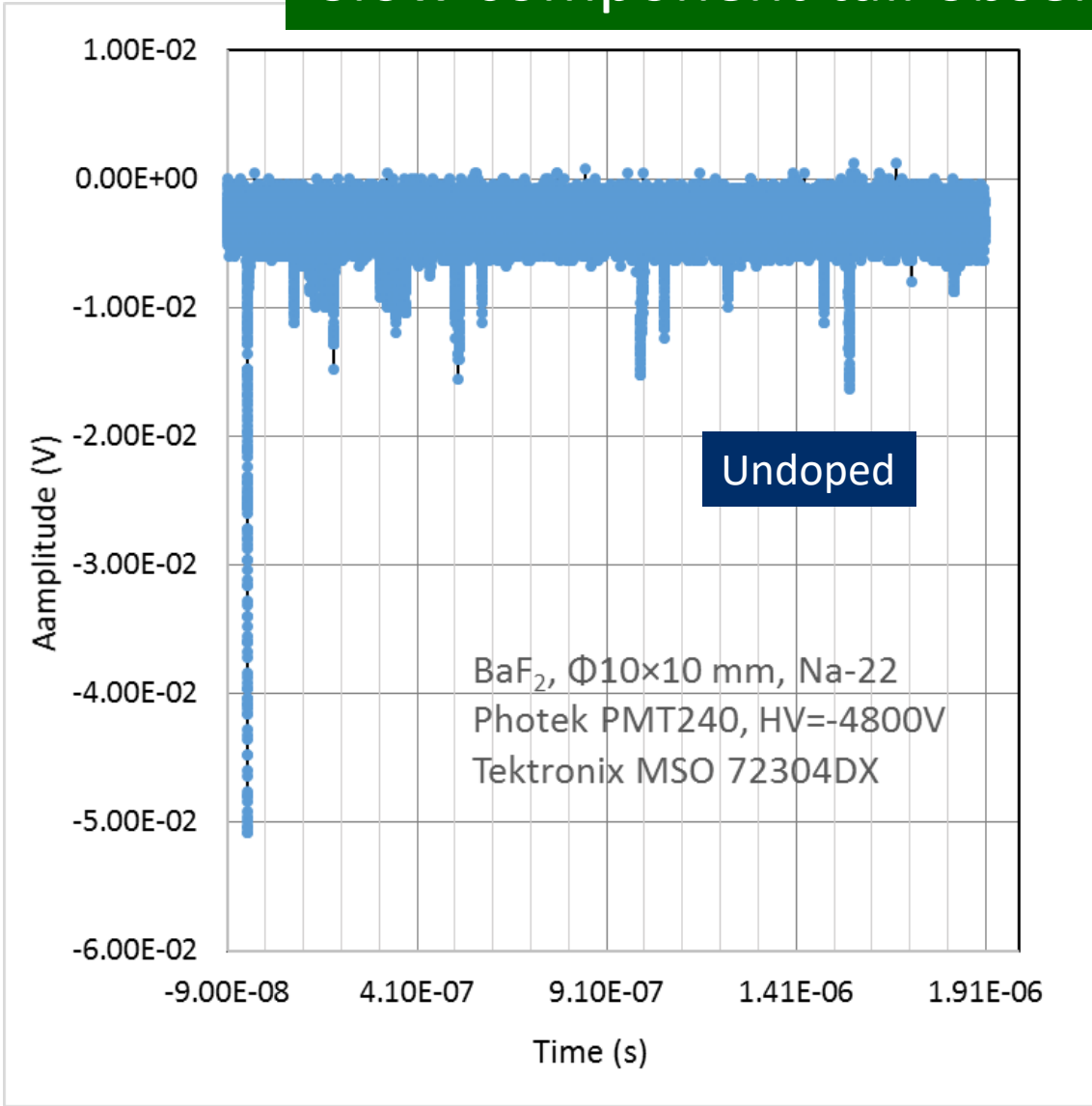




# Scintillation Pulse Tail Reduced in BaF<sub>2</sub>:Y



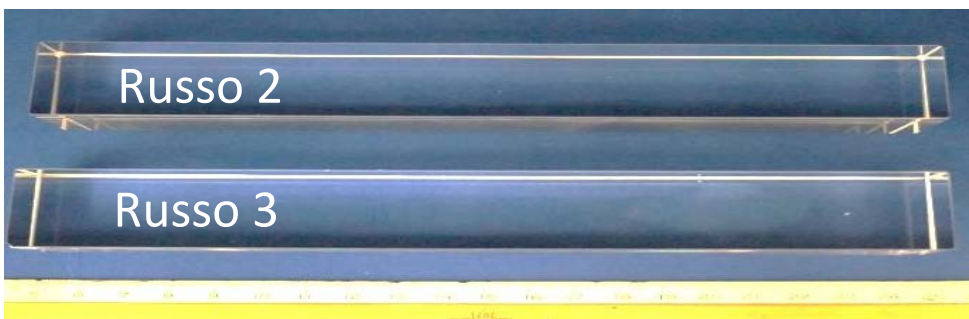
Slow component tail observed in 2 μs in BaF<sub>2</sub>, not BaF<sub>2</sub>:Y







# BGRI/Incrom/SIC BaF<sub>2</sub> Crystals



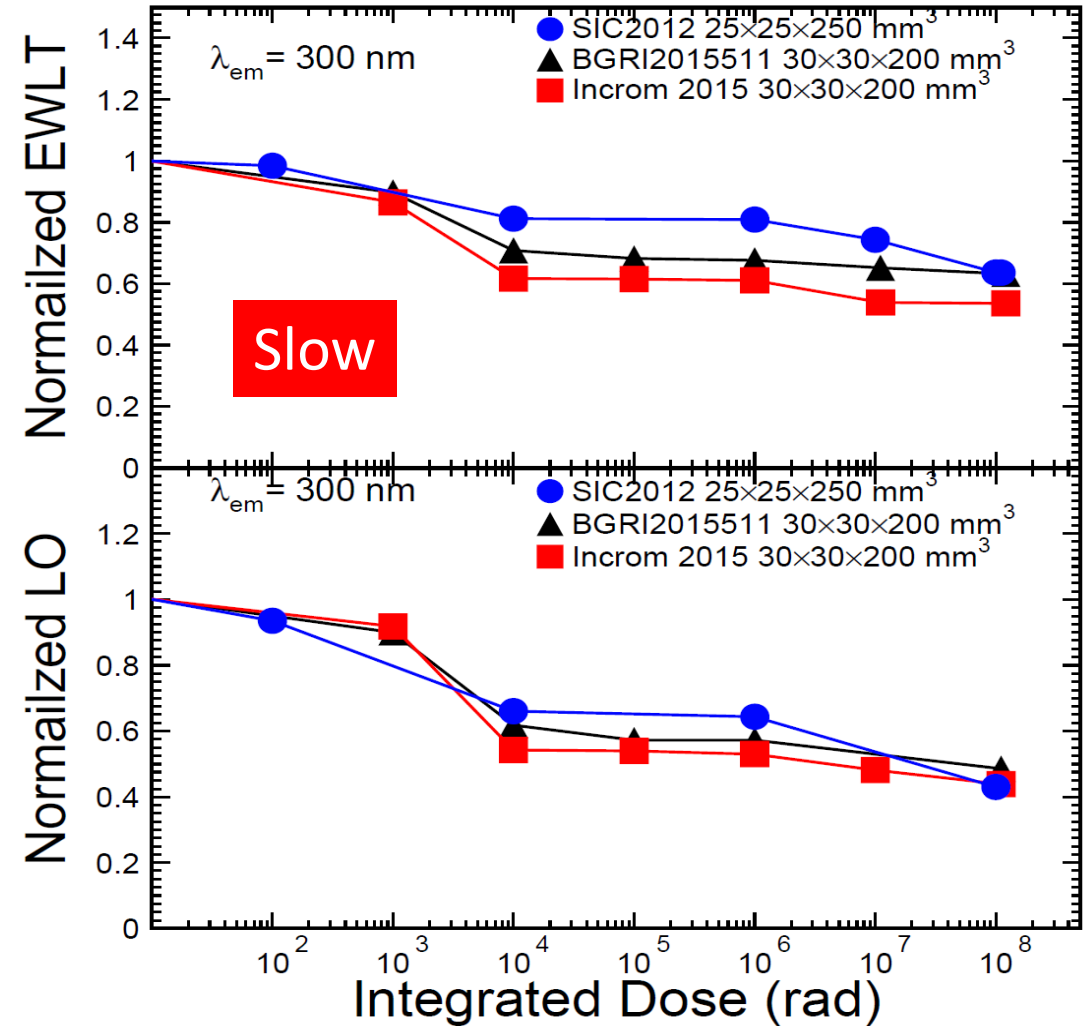
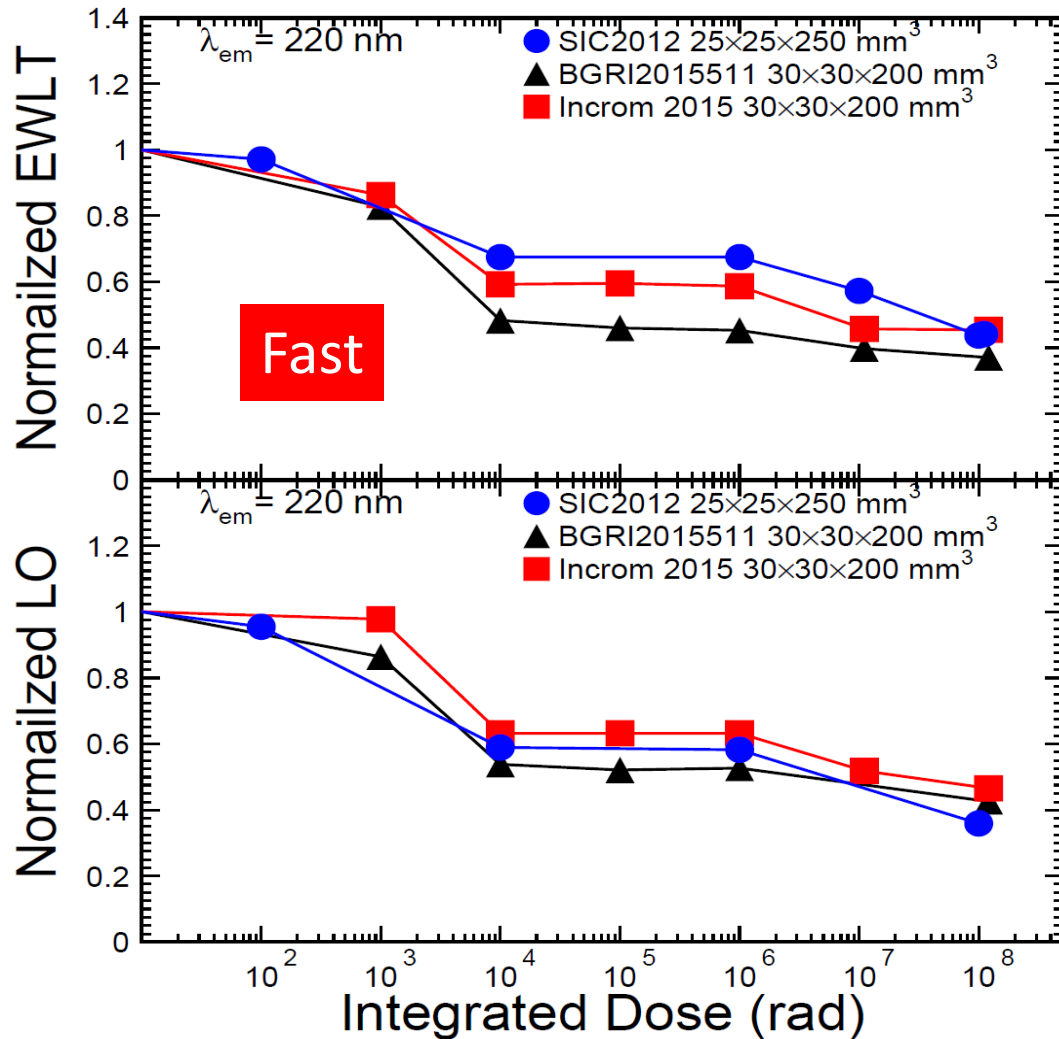
ID	Vendor	Dimension (mm <sup>3</sup> )	Polishing
SIC 1-20	SICCAS	30x30x250	Six faces
BGRI-2015 D, E, 511	BGRI	30x30x200	Six faces
Russo 2, 3	Incrom	30x30x200	Six faces



# $\gamma$ -Ray Induced Damage in $\text{BaF}_2$



Consistent damage in crystals from three vendors



Remaining light output after 120 Mrad: 40%/45% for the fast/slow component

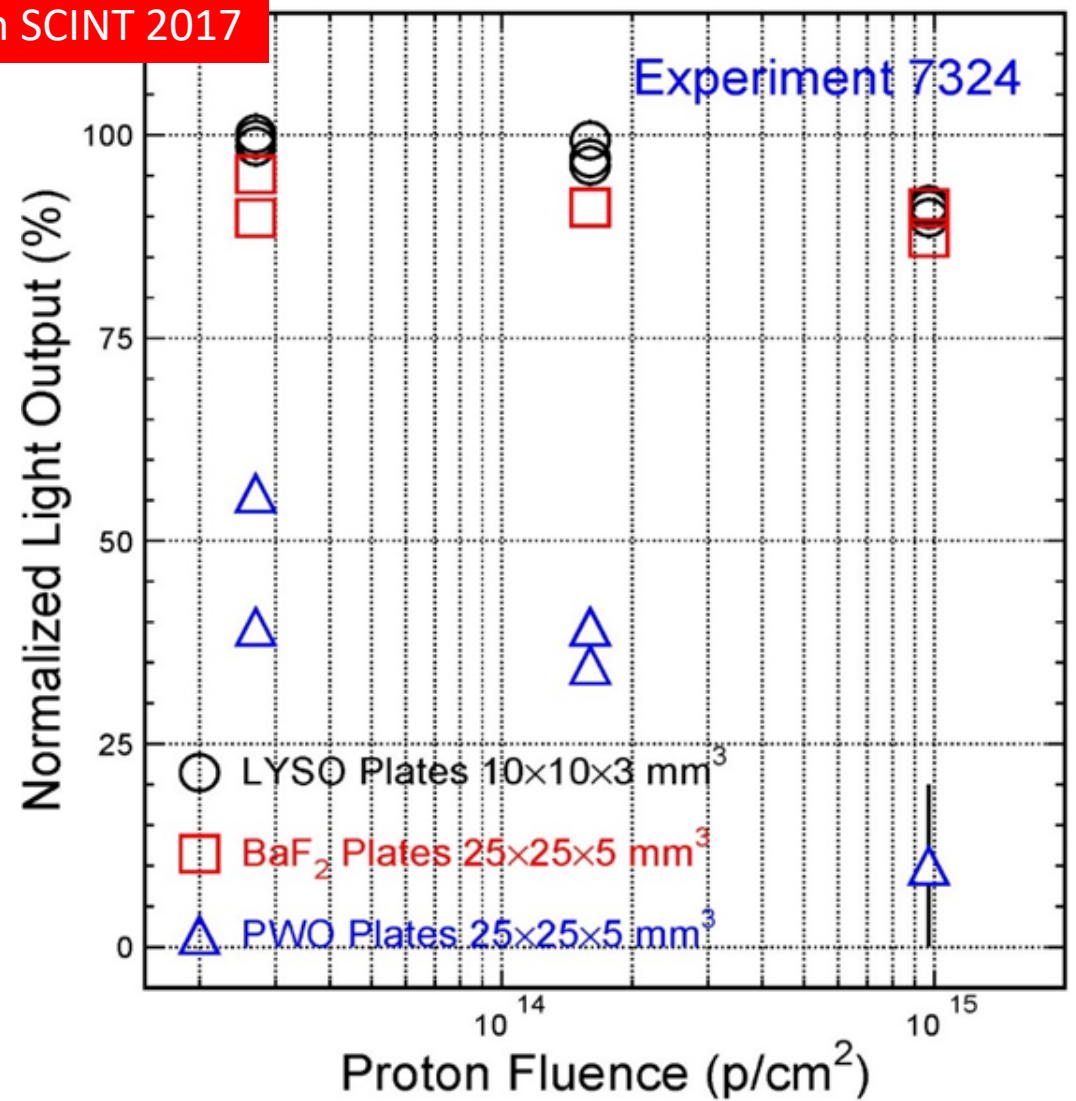
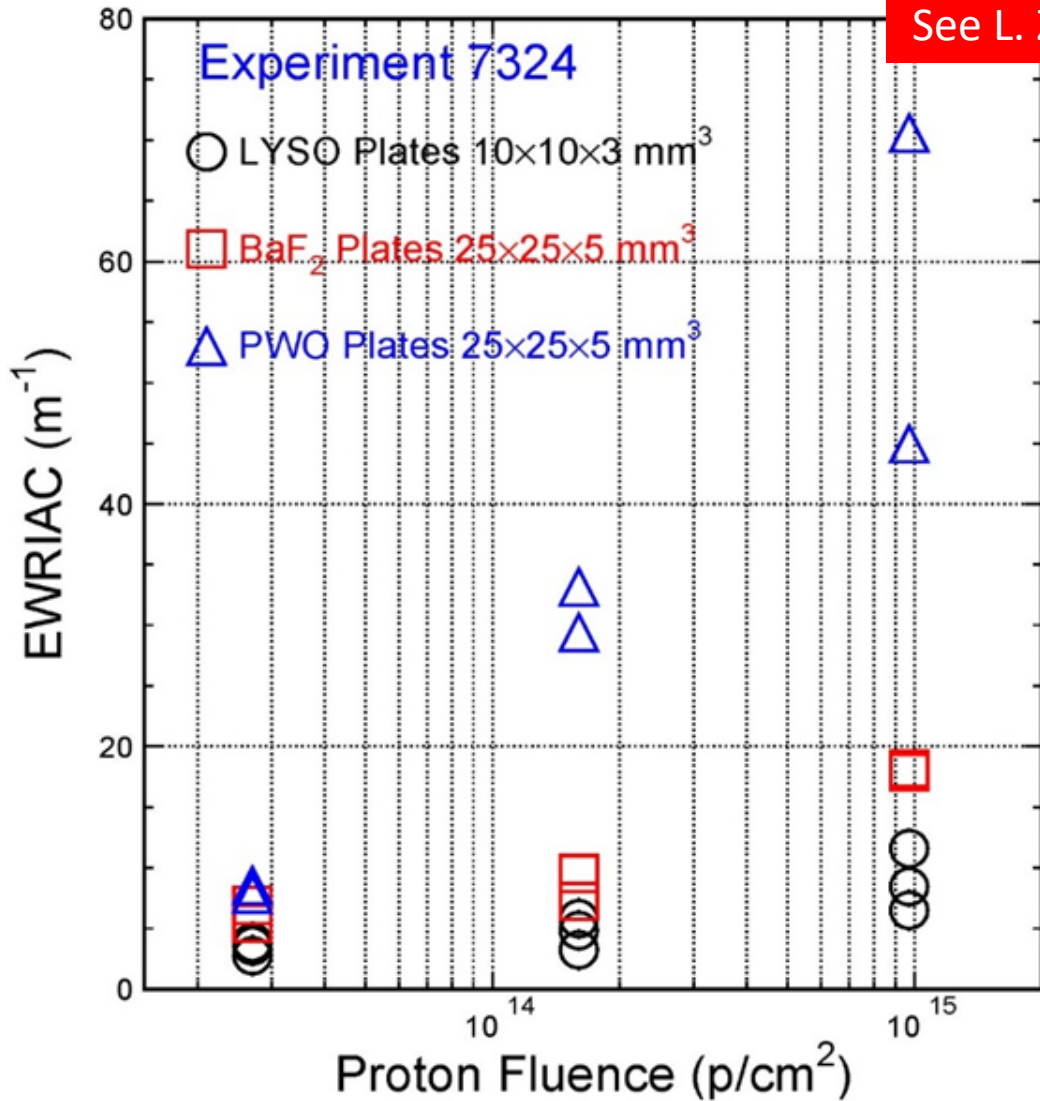


# Proton Damage in LYSO/BaF<sub>2</sub>/PWO



Excellent radiation hardness of LYSO and BaF<sub>2</sub> up to 10<sup>15</sup> p/cm<sup>2</sup>

See L. Zhang in SCINT 2017



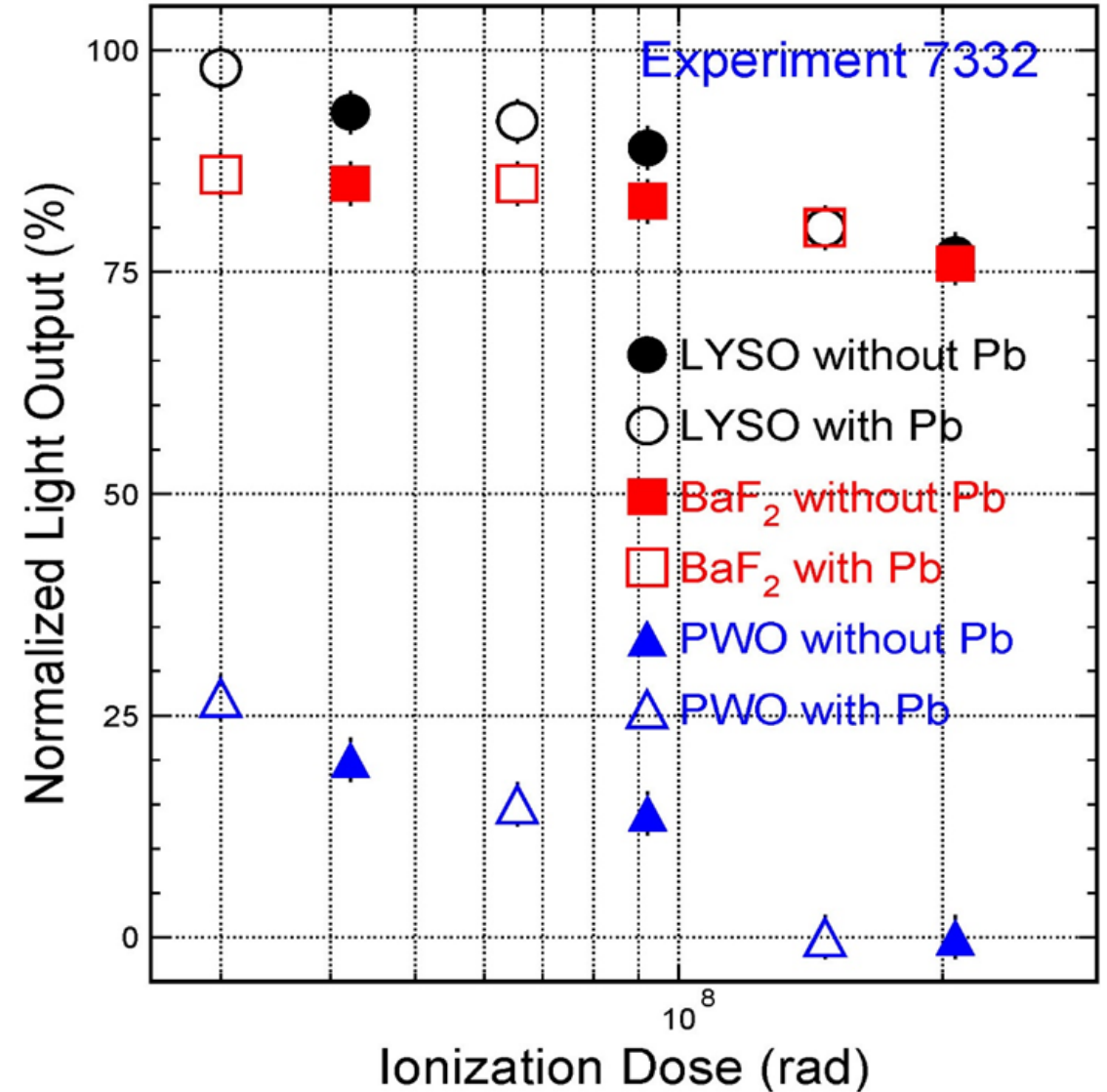
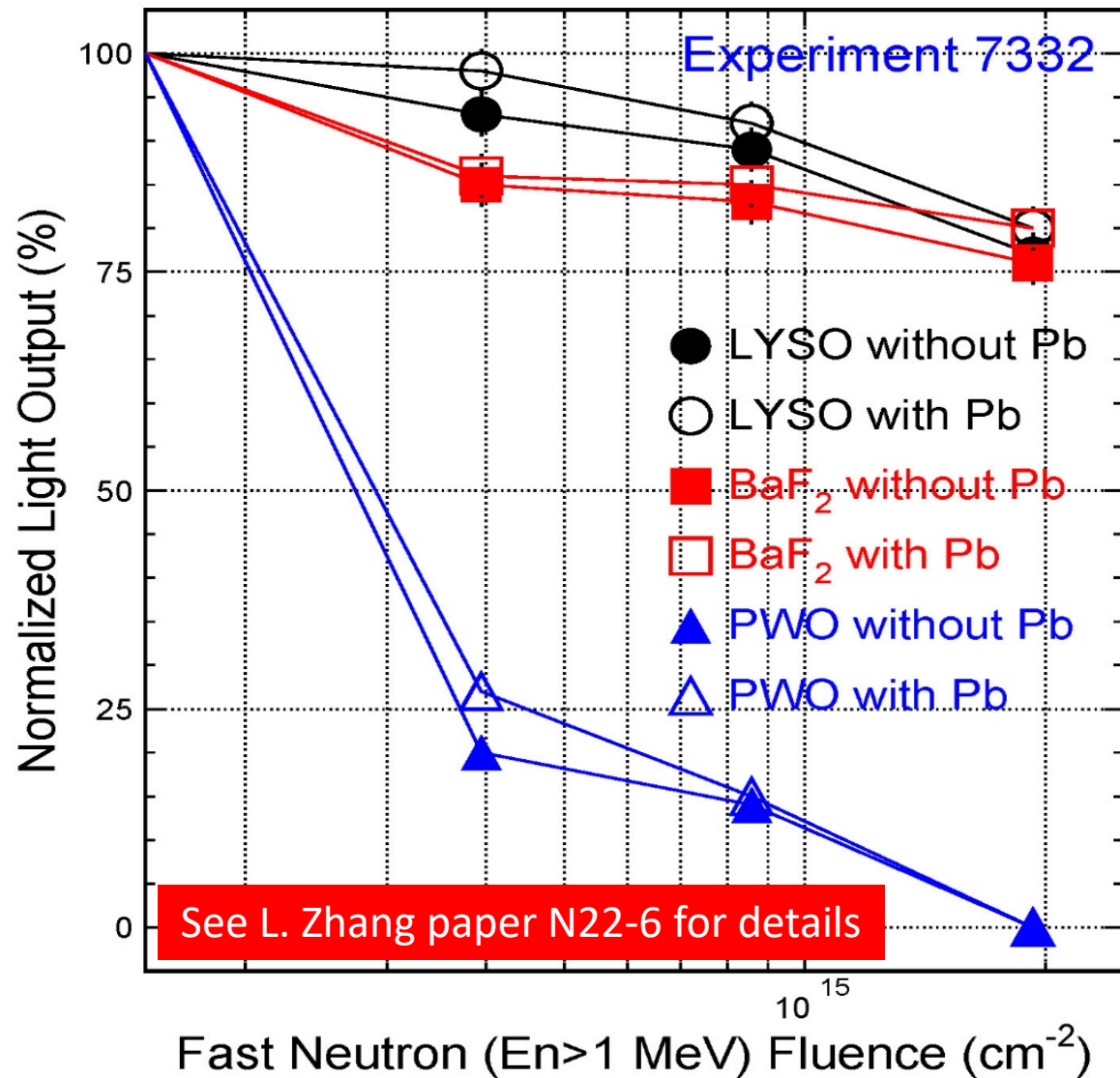




# Neutron Damage in LYSO/BaF<sub>2</sub>/PWO



Robust LYSO and BaF<sub>2</sub>: up to 200 Mrad and  $2 \times 10^{15}$  n/cm<sup>2</sup> & no neutron damage





# Summary



**LYSO and BaF<sub>2</sub> crystals show excellent radiation hardness beyond 100 Mrad,  $1 \times 10^{15}$  p/cm<sup>2</sup> and  $2 \times 10^{15}$  n/cm<sup>2</sup>. They will survive a severe radiation environment, such as the HL-LHC.**

**Undoped BaF<sub>2</sub> crystals provide fast light with sub-ns FWHM pulse width. Recently, yttrium doping increases its F/S ratio from 1/5 to 6/1 while maintaining its fast component intensity. At this level, its fast component and Fast/slow is similar to and less than undoped CsI. This material is proposed to Mu2e-II and Marie. It may also be considered for the CMS MTD barrel sensor.**

**We plan to optimize Y:BaF<sub>2</sub> further and test its radiation hardness. Will also pay an attention to DUV photodetectors: LAPPD, Si (Hamamatsu S13370 with 25% PDE at 200 nm) or diamond based solid state detector.**

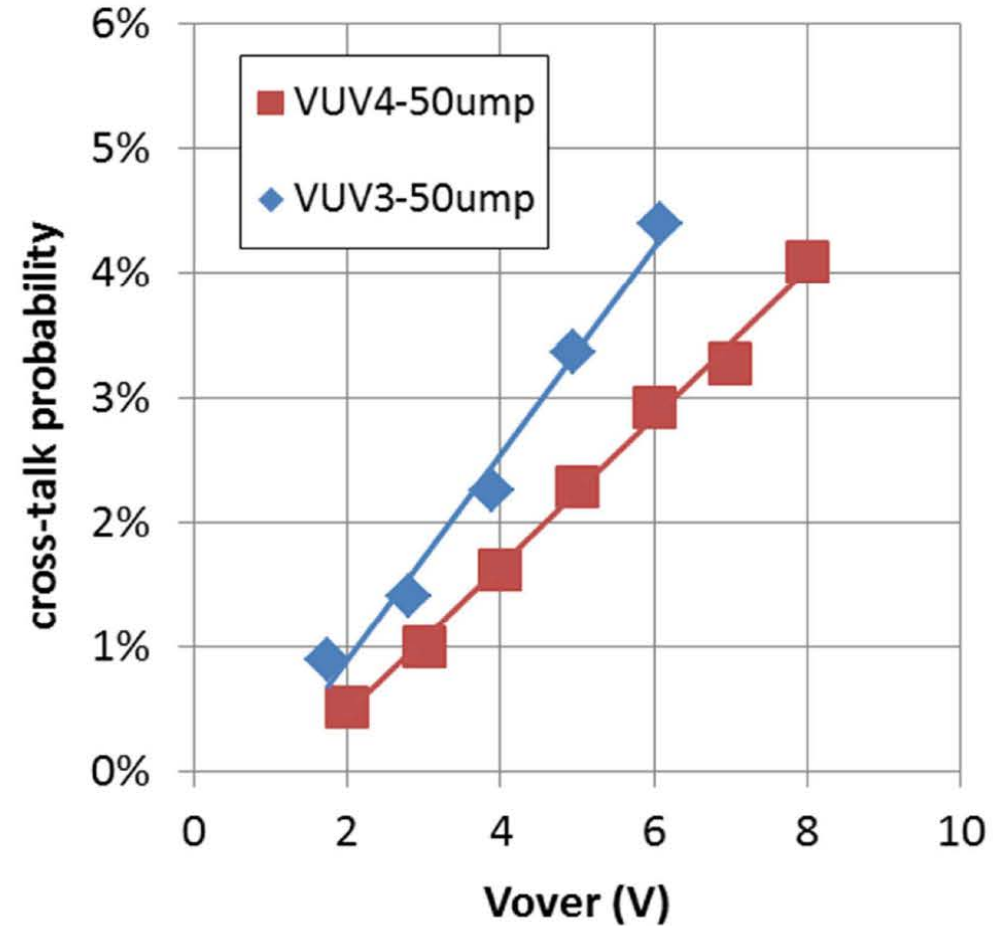
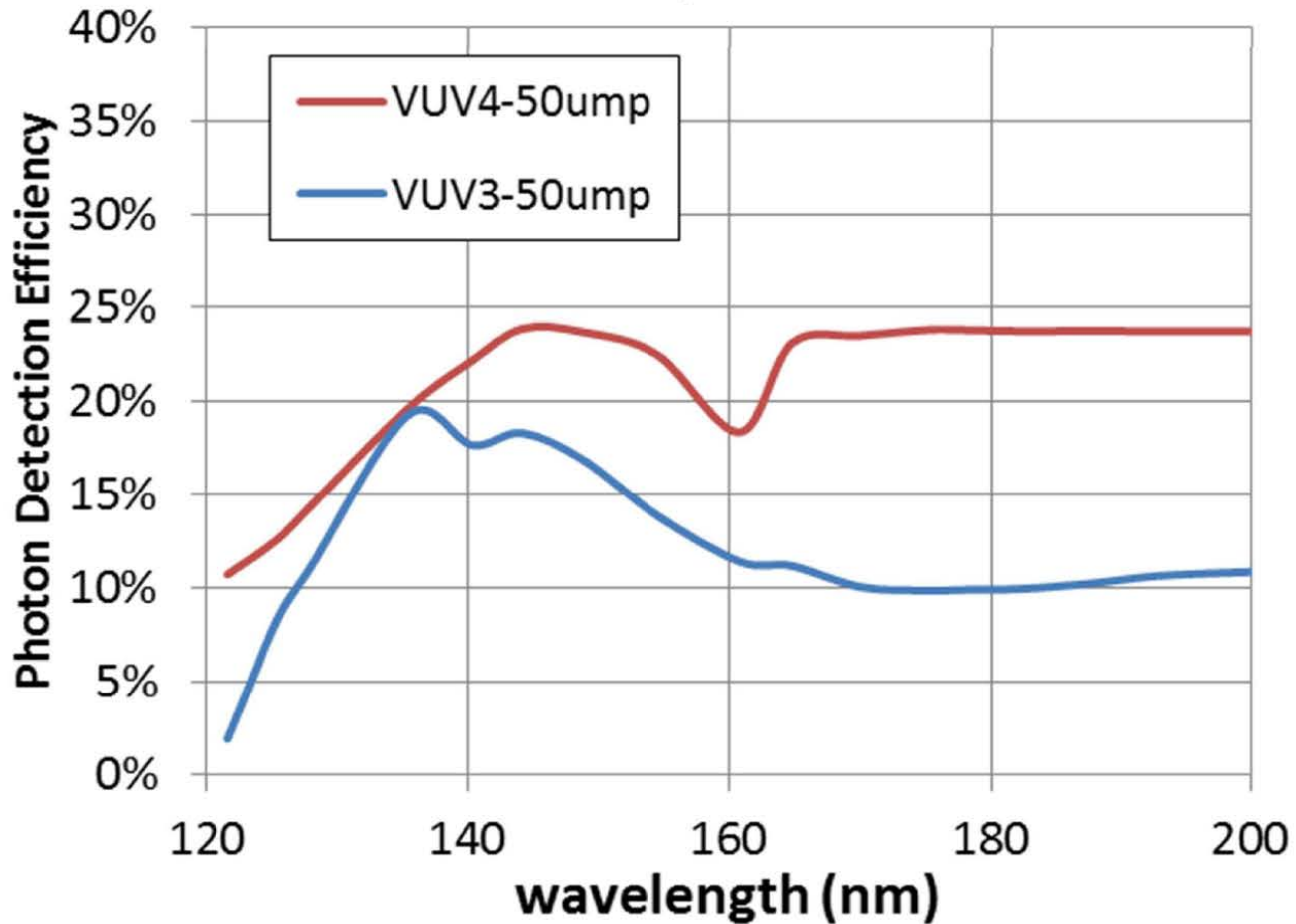


# Hamamatsu S13370 VUV SiPM



VUV-4 has a much better performance than VUV3

PDE measurement data  
Vover = 4V, in vacuum





# Diamond Photodetector



E. Monroy, F. Omnes and F. Calle, "Wide-bandgap semiconductor ultraviolet photodetectors, IOPscience 2003 Semicond. Sci. Technol. 18 R33

E. Pace and A. De Sio, "Innovative diamond photo-detectors for UV astrophysics", Mem. S.A.It. Suppl. Vol. 14, 84 (2010)

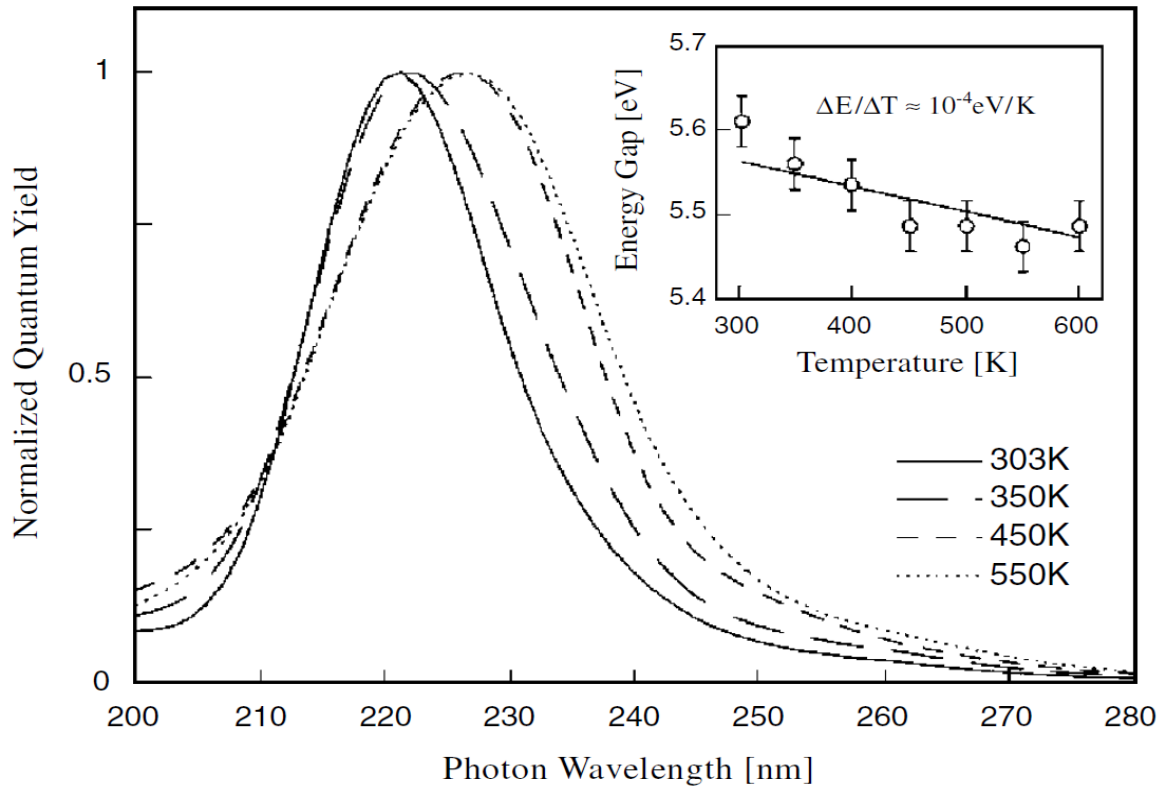


**Figure 6.** Quantum efficiency of diamond photoconductors at different temperatures and Arrhenius plot of the peak value (inset). (From [Sal00].)

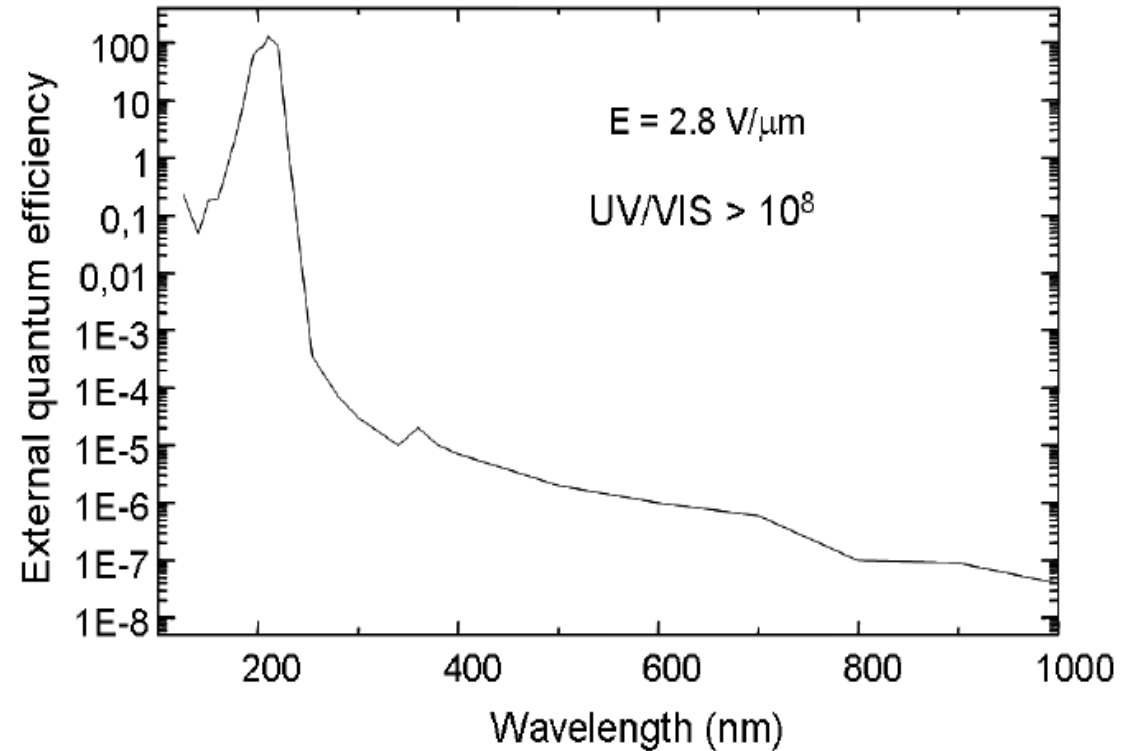


**Fig.4.** External quantum efficiency extended to visible and near infrared wavelength regions. The